

Steady-State and Time-Resolved Studies of the Photocleavage of Lysozyme by Co(III) Complexes

Thota Jyotsna and Challa V. Kumar*

Department of Chemistry, University of Connecticut, Storrs, Connecticut 06269-3060

Steffen Jockusch and Nicholas J. Turro

Department of Chemistry, Columbia University, New York, New York 10027

Received July 16, 2009. Revised Manuscript Received September 24, 2009

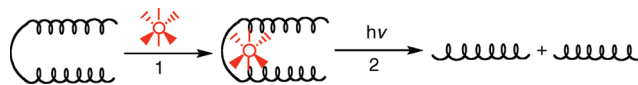
Steady-state and time-resolved studies of site-selective photocleavage of lysozyme by cobalt(III) complexes $[\text{Co}(\text{NH}_3)_5\text{Br}]^{2+}$ and $[\text{Co}(\text{NH}_3)_4\text{CO}_3]^+$ are reported. Photocleavage resulted in two fragments of molecular masses ~ 10.5 kDa and ~ 3.5 kDa, and the yield increased (8–33%) with irradiation time (0.16–0.8 h) as well as with the metal complex concentration (0.1–5 mM). The reaction proceeded to a significant extent even when nearly stoichiometric amounts of the reagents were used. Photocleavage was effective at wavelengths ranging from 310 to 390 nm, and cleavage was inhibited by the addition of selected metal ions such as Gd(III) at moderate concentrations (2 mM). Gd(III) is known to bind at Asp52/Glu35 residues on lysozyme, and these residues are located at the enzyme active site. Current and previous studies suggest that Co(III) metal complexes bind at this site on lysozyme. Consistent with this hypothesis, $[\text{Co}(\text{NH}_3)_4\text{CO}_3]^+$ (8 mM) inhibited lysozyme activity by 67%. Laser flash photolysis studies show that excitation of the metal complexes $[\text{Co}(\text{NH}_3)_5\text{Br}]^{2+}$ and $[\text{Co}(\text{NH}_3)_4\text{CO}_3]^+$ (308 nm, 20 ns pulse width) resulted in the corresponding ligand-derived radical intermediates. For example, photoexcitation of an aqueous solution of $[\text{Co}(\text{NH}_3)_5\text{Br}]^{2+}$ at 308 nm resulted in the formation of $\text{Br}_2^{\cdot -}$. When the excitation was carried out in the presence of lysozyme, $\text{Br}_2^{\cdot -}$ was quenched with a bimolecular rate constant of $1.4 \times 10^9 \text{ M}^{-1} \text{ s}^{-1}$. Quenching resulted in protein-derived radicals ($\text{Trp}^{\cdot +}$ and $\text{Tyr}^{\cdot +}$), as identified by their characteristic known transient absorption bands. Steady-state studies correlated with the time-resolved data, and taken together, these illustrated the reactivities of Co(III) metal complexes to direct protein photocleavage with high selectivity.

Introduction

Numerous enzymes and proteins require metal ions for their biological function, and identification of the metal binding sites on biomolecules is essential for understanding their metallo-biochemistry. However, identification of these metal binding sites is challenging and requires single-crystal X-ray diffraction (XRD) studies or detailed NMR experiments.¹ Therefore, alternative approaches for the identification of metal binding sites is highly desirable. In this context, photochemical approaches are promising. One significant advantage of photochemical reactions is that detailed mechanistic information can be obtained by conducting time-resolved studies. Previous work from this laboratory² and others³ have demonstrated photochemical approaches to footprint ligand binding sites as well as metal binding sites on proteins.

Photoactive metal species such as vanadate,⁴ uranyl⁵ and Fe(III)⁶ are known to cleave proteins upon activation by light. Vanadate, a metal-oxo ion, is isosteric to phosphate and often binds at phosphate binding sites on proteins and photocleaves the peptide backbone. In contrast, uranyl binds to Ni(II) binding sites on serum albumins and photocleaves the protein backbone at the corresponding metal binding sites. Recently, uranyl was used to footprint protein phosphorylation sites on proteins, where uranyl has been proposed to bind to phosphate groups of proteins.⁷

Scheme 1. A General Strategy for the Photochemical Footprinting of Metal Binding Sites on Proteins



Our current strategy is outlined in Scheme 1. A transition metal complex is designed to bind at the desired metal binding site (step 1), and the protein-bound metal complex is then photoactivated to cleave the protein backbone at or near the binding site (step 2).¹³ Identification of the photocleavage products by standard biochemical methods reveals the binding site of the metal complex, and the metal binding site can be deduced from these data. Competitive inhibition of the protein photocleavage by the presence of specific metal ions confirms that the metal complex indeed cleaves the protein at the intended site. This simple strategy is evaluated here, in steady-state and time-resolved studies.

*Corresponding author. E-mail: Challa.Kumar@uconn.edu.

(1) *Physical Methods in Bioinorganic Chemistry*; Que, L., Ed.; University Science Books: Minneapolis, MN, 2000.

(2) (a) Kumar, C. V.; Buranaprapuk, A. *Angew. Chem.* **1997**, *36*, 2085. (b) Kumar, C. V.; Buranaprapuk, A.; J. Opitck, G.; Moyer, M. B.; Jockusch, S.; Turro, N. J. *Proc. Natl. Acad. Sci. U.S.A.* **1998**, *95*, 10361. (c) Buranaprapuk, A.; Kumar, C. V.; Jockusch, S.; Turro, N. J. *Tetrahedron* **2000**, *56*, 7019. (d) Kumar, C. V.; Buranaprapuk, A.; Sze, H. *Chem. Commun.* **2001**, 297. (e) Kumar, C. V.; Buranaprapuk, A.; Thota, J. *Proc. Natl. Acad. Sci. (India): Chem. Sci.* **2002**, *114*, 579.

(3) (a) Jackson, G. S.; Murray, I.; Hosszu, L. L. P.; Gibbs, N.; Waltho, J. P.; Clarke, A. R.; Collinge, J. *Proc. Natl. Acad. Sci. U.S.A.* **2001**, *98*, 8531. (b) Ngoka, L. C. M.; Gross, M. L. *J. Mass Spectrom.* **2000**, *35*, 265.

(4) (a) Correia, J. J.; Lipscomb, L. D.; Dabrowiak, J. C.; Isern, N.; Zubietta, J. *Arch. Biochem. Biophys.* **1994**, *309*, 94. (b) Crans, D. C.; Sudhakar, K.; Zamborelli, T.; Rehder, D. *Angew. Chem., Int. Ed.* **1991**, *30*, 148. (c) Cremon, C. R.; Loo, J. A.; Edmonds, C. G.; Hatlelid, K. M. *Biochemistry* **1992**, *31*, 491.

(5) Duff, M. R., Jr.; Kumar, C. V. *Angew. Chem., Int. Ed. Engl.* **2006**, *45*, 137.

(6) (a) Moczek, G.; Tang, W.-J. Y.; Gibbons, I. R. *J. Cell Biol.* **1988**, *106*, 1607.

(b) Moczek, G.; Gibbons, I. R. *J. Biol. Chem.* **1990**, *265*, 2917. (c) Moczek, G.; Farias, J.; Gibbons, I. R. *Biochemistry* **1991**, *30*, 7225.

(7) Kristensen, L. H.; Nielsen, P. E.; Joergensen, C. I.; Kragelund, B. B.; Moellegaard, N. E. *ChemBioChem* **2008**, *9*, 2377.

Chart 1. The Structures of Co(III) Hexamine and Its Derivatives

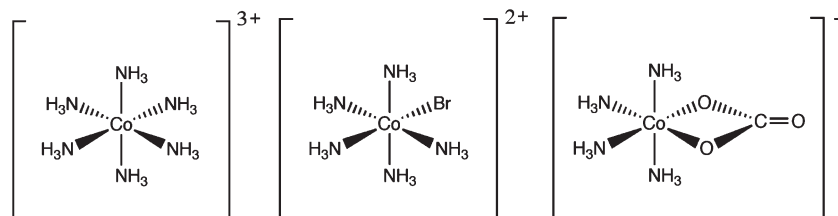
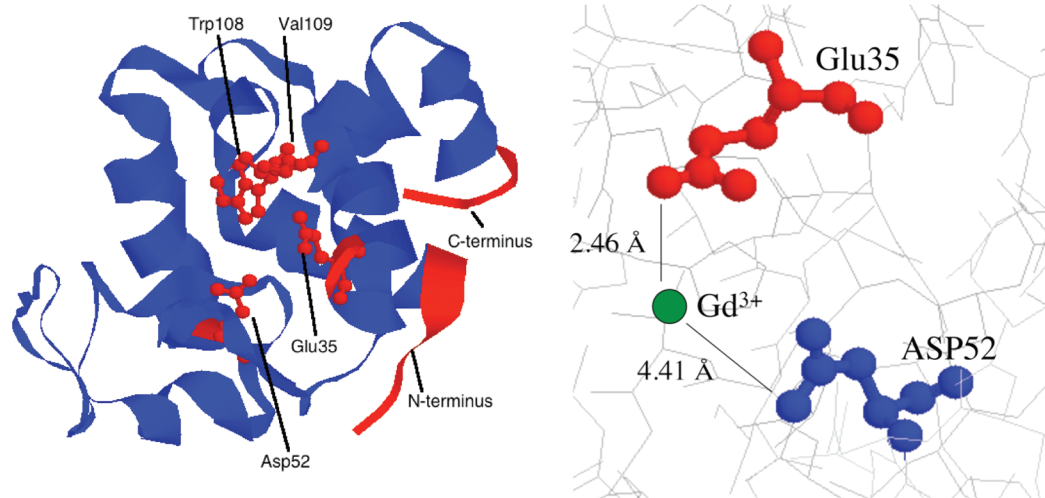


Chart 2. (Left) Three-Dimensional Structure of Lysozyme, Highlighting the Locations of Some Important Residues; (Right) Binding of Gd(III) at the Active Site Residues, Asp52/Glu35 (Bold Residues)

17



Co(III) ammine complexes are the focus of this paper, and these bind to particular sites on several proteins.⁸ Photoexcitation into the ligand-to-metal charge transfer (LMCT) bands of Co(III) complexes (Chart 1) generates ligand radicals,^{9–12} and these radicals have the potential to cleave the protein backbone. By adjusting the size, reactivity, and the type of ligands, the structure of the Co(III) complexes can be adjusted to target appropriate sites on proteins.

In support of the above strategy, several Co(III) complexes were shown to photocleave several proteins,¹³ and here we examined the key mechanistic steps of the lysozyme photocleavage by steady-state and flash photolysis studies. Lysozyme is a small (molecular weight ~14.3 kDa),¹⁴ inexpensive, water-soluble hydrolytic enzyme,¹⁵ and the active site of lysozyme is located in a cleft, which is lined with polar groups.¹⁶

For example, Glu35 is one of the residues in the active site, and this residue is critical for the catalytic activity of the enzyme; Asp52 is another polar residue located within 6 Å from Glu35.

Metal ions such as Mn(II), Co(II), Gd(III), Ni(II), and lanthanide ions bind to lysozyme at Glu35/Asp52 (Chart 2).^{18–22} Crystal structure of lysozyme indicates that these residues are readily accessible from the solvent, and the open space around Glu35/Asp52 site can accommodate small metal complexes such as the ones shown in Chart 1, via outer sphere interactions. Here, the steady-state and flash photolysis studies of lysozyme photocleavage by two Co(III) complexes are reported.

Experimental Section

Materials. Chicken hen egg lysozyme was purchased from Sigma (St. Louis, MO), while the metal complexes, pentamminebromocobalt(III) bromide $[\text{Co}(\text{NH}_3)_5\text{Br}]^{2+}$, and tetramminecarbonatocobalt(III) nitrate $[\text{Co}(\text{NH}_3)_4\text{CO}_3]^+$, were synthesized by following reported methods.²³ The electronic absorption spectra of the complexes are $[\text{Co}(\text{NH}_3)_5\text{Br}]^{2+}$ [263 nm ($18\,500\text{ M}^{-1}\text{ cm}^{-1}$), 550 nm ($55\text{ M}^{-1}\text{ cm}^{-1}$)] and $[\text{Co}(\text{NH}_3)_4\text{CO}_3]^+$

(8) (a) Kim, S.; Cowan, J. A. *Inorg. Chem.* **1992**, *31*, 3495. (b) Kucharski, L.; Lubbe, W. J.; Maguire, M. E. *J. Biol. Chem.* **2000**, *275*, 16767. (c) Jou, R.; Cowan, J. A. *J. Am. Chem. Soc.* **1991**, *113*, 6685.

(9) Basolo, F.; and Pearson, R. G. In *Mechanisms of Inorganic Reactions: A Study of Metal Complexes in Solution*; John Wiley: New York, 1967; p 158.

(10) Stadtman, E. R.; Levine, R. L. *Amino Acids* **2003**, *25*, 207.

(11) Balzani, V.; Carassiti, V. In *Photochemistry of Coordination Compounds*; Academic Press: New York, 1970.

(12) (a) Hoffman, M. Z.; Olson, K. R. *J. Phys. Chem.* **1978**, *82*, 2631. (b) Penkett, S. A.; Adamson, A. W. *J. Am. Chem. Soc.* **1965**, *87*, 2514. (c) Grossweiner, L. I.; Matheson, M. S. *J. Phys. Chem.* **1957**, *61*, 1089. (d) Chen, S.; Cope, V. W.; Hoffman, M. Z. *J. Phys. Chem.* **1973**, *77*, 1111.

(13) (a) Kumar, C. V.; Thota, J. *Inorg. Chem.* **2005**, *44*, 825. (b) Thota, J.; Bandara, K.; Kumar, C. V. *Photochem. Photobiol. Sci.* **2008**, *7*, 1531.

(14) Weiss, M. S.; Palm, G. J.; Hilgenfeld, R. *Acta Crystallogr., Sect. D.* **2000**, *56*, 952.

(15) Teichberg, V. I.; Sharon, N.; Moulton, J.; Smilansky, A.; Yonath, A. *J. Mol. Biol.* **1974**, *87*, 357.

(16) Kortvelyesi, T.; Silberstein, M.; Dennis, S.; Vajda, S. *J. Comput.-Aided Mol. Des.* **2003**, *17*, 173.

(17) (a) Kurachi, K.; Sieker, L. C.; Jensen, L. *J. Biol. Chem.* **1975**, *250*, 7663. (b) Hunter, T. M.; McNae, I. W.; Simpson, D. P.; Smith, A. M.; Moggach, S.; White, F.; Walkinshaw, M. D.; Parsons, S.; Sadler, P. J. *Chemistry* **2007**, *13*, 40.

(18) Ikeda, K.; Hamaguchi, K. A. *J. Biol. Chem.* **1973**, *248*, 307.

(19) Pesek, J. J.; Schneider, J. F. *J. Inorg. Biochem.* **1988**, *32*, 233.

(20) (a) Kurachi, K.; Sieker, L. C.; Jensen, L. H. A. *J. Biol. Chem.* **1975**, *250*, 7663. (b) Olmo, R.; Huerta, P.; Blanco, D.; Teijon, J. M. *J. Inorg. Biochem.* **1992**, *47*, 89.

(21) Norton, R. S.; Allerhand, A. *J. Biol. Chem.* **1977**, *252*, 1795.

(22) Li, S. J. *Biopolymers* **2006**, *81*, 74.

(23) (b) Schlessinger, G. G. *Inorganic Syntheses IX*; McGraw-Hill Company: New York; 1967.

Table 1. Quantum Yields for the Photoreduction of Co(III) Complexes

complex	Co(III) photoreduction quantum yields			
	254 nm	370 nm	410 nm	550 nm
[Co(NH ₃) ₆] ³⁺	0.16 ²⁷	0 ²⁷		
[Co(NH ₃) ₅ Br] ²⁺	0.19 ²⁸	0.15 ²⁹	0.071 ²⁹	0.0014 ²⁸
[Co(NH ₃) ₄ CO ₃] ⁺	0.06 ³⁰			

[238 nm, and 520 nm (104 M⁻¹ cm⁻¹)], and the FTIR spectra of the samples matched those reported.^{11,24–26} Photoreduction quantum yields of Co(III) complexes at key wavelengths, where the ligand served as the reductant, are given in Table 1. Note that photoreduction of the metal center was demonstrated at specific wavelengths, in particular cases.

Photocleavage Reactions. Photocleavage was carried out at room temperature in Tris buffer (10 mM Tris HCl, pH 7.0) or in deionized water (pH 5), under air-saturated conditions, as described earlier.² Briefly, a mixture of the protein (75 μM) and the Co(III) complex (0.6–5 mM, 200 μL) was irradiated at 310 nm, or longer wavelengths, using a monochromatic light source (PTI power supply, 150-W Xenon lamp, PTI model A1010 monochromator). Average light intensity emitted by the source at a given wavelength was measured by ferrioxalate actinometry,³¹ and with the above lamp-setup, the monochromator tuned to 344 nm, the sample was exposed to 3.2 ± 0.04 × 10⁻⁸ einsteins/min. Irradiated samples were dried in a Speedvac (Savant Integrated System ISS10) for storage or for subsequent studies.

Electrophoresis. The photoreaction mixture was analyzed by sodium dodecylsulfate (SDS)/polyacrylamide gel electrophoresis (PAGE), as described previously.³² High-quality images of the protein gels were obtained by scanning the dye-stained gels with a Umax Astra 1220U scanner. Band intensities were quantified using NIH image software (v. 1.63), and product yields were estimated (yield of band I = intensity of band I / (intensity of band I plus that of the unreacted lysozyme)). Intensities of individual bands varied by ± 5% from gel to gel, due to precipitation problems, and therefore values from 2 to 3 gels were used to calculate average yields. The distance of migration of the protein band depended linearly on the logarithm of protein molecular mass.³³ The molecular masses of the photofragments were assessed from calibration graphs constructed using proteins of known molecular masses.

Lysozyme Activity Studies. Glycol chitin (6 mM) was reacted with lysozyme (20 μM) in deionized water, pH 5, at 37 °C overnight, with different concentrations of [Co(NH₃)₄CO₃]⁺ (0, 2, 4, or 8 mM). A solution of K₃Fe(CN)₆ (1.8 mM) was added to the reaction mixture and heated at 100 °C for 10 min, and absorbance due to the conversion of Fe(III) to Fe(II) was measured at 420 nm. Calibration graphs were constructed using *N*-acetyl glucosamine. The extent of enzyme inhibition (%) was calculated by measuring the change in absorbance at 420 nm in the presence versus the absence of the metal complex. In control studies, Co(III) complexes did not have any influence on the concentrations of Fe(III) or Fe(II), and absorbance due to the Co(III) complexes at 420 nm, if any, was subtracted accordingly.

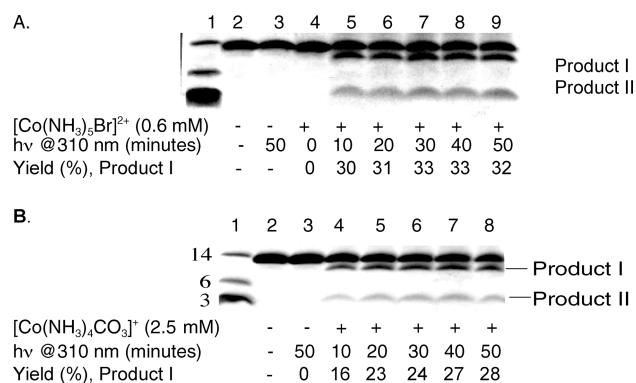


Figure 1. Lysozyme photocleavage by Co(III) complexes (10 mM Tris HCl, pH 7.0, 310 nm irradiation, 10–50 min) resulted in two fragments. Molecular weight markers from the top to the bottom in lane 1 are 14, 6, and 3.5 kDa, and the other lanes are as marked. Lysozyme (75 μM) photocleavage, as a function of irradiation time, by (A) [Co(NH₃)₅Br]²⁺ (0.6 mM) and (B) [Co(NH₃)₄CO₃]⁺ (2.5 mM).

Laser Flash Photolysis. These experiments were carried out by an apparatus described previously.³⁴ Laser pulses from an excimer laser (Lextra 50, Lambda Physik, 308 nm, 50 mJ/pulse, 20 ns pulse duration) were used to excite the samples, and absorbance changes, subsequent to excitation, were monitored with a pulsed 150 W xenon lamp and an ISA H10 monochromator. The signals from a Hamamatsu R928 photomultiplier tube were recorded with a Tektronix TDS 380 (400 MHz bandwidth) programmable digitizer. This digitizer was controlled along with other aspects of the experiment (shutters, lamp pulser, monochromator, etc.) through a GPIB interface board (National Instruments NBGPIB) using a Macintosh G3 with Labview 5 software (National Instruments). Kinetic traces were monitored at specific wavelengths, and the transient absorption spectra at specific delay times were constructed from these traces.

Results and Discussion

Steady-state and time-resolved studies on protein photocleavage by Co(III) complexes indicated that ligand-derived radicals are primarily responsible for the peptide fragmentation, and details of our investigations are described below:

Photocleavage Studies. Irradiation of a mixture of lysozyme and [Co(NH₃)₅Br]²⁺ at 310 nm and subsequent analysis of the reaction mixture by SDS PAGE (Figure 1) indicated a pair of product bands that migrated faster than the starting material. By using the known molecular weight markers (lane 1), and construction of a calibration graph, we found that the approximate molecular masses of the product bands (lanes 5–9) are 10.5 and 3.5 kDa. These masses roughly add-up to that of the unreacted lysozyme (14.3 kDa), and the molecular masses of the product bands matched with those previously reported.¹³ The pair of bands suggests that the daughter fragments may arise from a single cut in the parent molecule.

Extensive nonspecific cleavage of the peptide backbone can be ruled out because indiscriminate photocleavage would have resulted in smearing of product bands in lanes 5–9. Incubation of a mixture of lysozyme and the metal complex in the dark, under similar conditions (lane 4) did not yield any fragmentation. Similarly, irradiation of lysozyme in the absence of the metal complex (lane 3) did not yield any products. Therefore, both light and the metal complex are essential for the observed photocleavage. The product yields increased only marginally (30–33%) as a function of irradiation time (10–50 min). Only two product

- (24) (a) Hill, D. G.; Rosenberg, A. F. *J. Chem. Phys.* **1954**, *22*, 148. (b) Svatos, G. F.; Sweeny, D. M.; Mizushima, S.; Curran, C.; Quagliano, J. V. *J. Am. Chem. Soc.* **1957**, *79*, 3313. (c) Kobayashi, M.; Fujita, J. *J. Chem. Phys.* **1955**, *23*, 1354. (d) Dasgupta, T. P.; Harris, G. M. *J. Am. Chem. Soc.* **1969**, *91*, 3207.
- (25) Yalman, R. G. *J. Am. Chem. Soc.* **1955**, *77*, 3219.
- (26) Adamson, A. W.; Sporer, A. *J. Am. Chem. Soc.* **1958**, *80*, 3865.
- (27) Manfrin, M. F.; Varani, G.; Moggi, L.; Balzani, V. *Mol. Photochem.* **1969**, *1*, 387.
- (28) Adamson, A. W.; Waltz, W. L.; Zinato, E.; Watts, D. W.; Fleischauer, P. D.; Lindholm, R. D. *Chem. Rev.* **1968**, *68*, 541.
- (29) Adamson, A. W. *Discuss. Faraday Soc.* **1960**, *29*, 163.
- (30) Cope, V. W.; Chen, S.; Hoffman, M. Z. *J. Am. Chem. Soc.* **1973**, *95*, 3116.
- (31) Hatchard, H. G.; Parker, C. A. *Proc. R. Acad. Sci. (London)*, **A** **1956**, *235*, 518.
- (32) Kumar, C. V.; Buranaprapuk, A. *J. Am. Chem. Soc.* **1999**, *121*, 4262.
- (33) Schagger, H.; Von Jagow, G. *Anal. Biochem.* **1987**, *166*, 368.

- (34) Yagci, Y.; Jockusch, S.; Turro, N. J. *Macromolecules* **2007**, *40*, 4481.

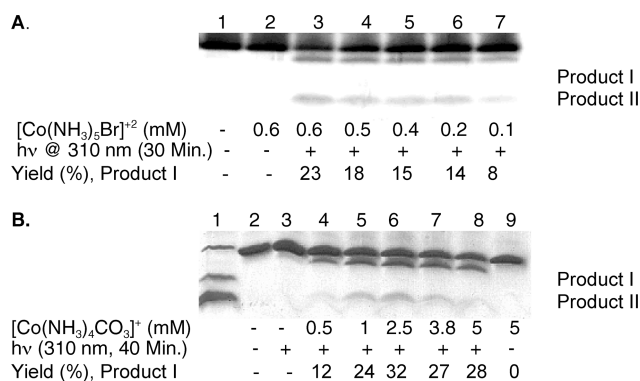


Figure 2. Photocleavage of lysozyme (75 μ M, 10 mM Tris HCl, pH 7.0, 310 nm irradiation) as a function of metal complex concentration. Lane 1 contains molecular weight markers (14, 6, and 3.5 kDa), and the other lanes are as marked. (A) Photocleavage by $[\text{Co}(\text{NH}_3)_5\text{Br}]^{2+}$, as a function of metal concentration (0–0.6 mM). (B) Photocleavage by $[\text{Co}(\text{NH}_3)_4\text{CO}_3]^+$ as a function of metal concentration (0–5 mM). Product formation with little or no change in selectivity is demonstrated.

bands are noted at all irradiation times, and hence selectivity of the photoreaction is independent of the irradiation time.

Irradiation of lysozyme (75 μ M) in the presence of $[\text{Co}(\text{NH}_3)_4\text{CO}_3]^+$ (2.5 mM) also resulted in protein photocleavage (Figure 1B), and the same pair of product bands appeared as in the case of the bromo-derivative. Yields of photoproduct improved with irradiation time, from 16 to 28% (10–50 min). Note that the reaction selectivity is unaltered as a function of irradiation time, the reaction is not limited to one metal complex, and the same pair product bands are noted with both the metal complexes.

In both cases, the addition of fresh metal complex to the irradiated reaction mixture and continued irradiation did not improve the product yields any further. One possibility is that the initial events in the photocleavage branch out to give chemically modified protein, which does not result in fragmentation of the backbone. In support of this assessment, mass spectrometry of lysozyme, isolated from the reaction mixture, indicated increase in molecular mass consistent with the addition of one, two, and up to five oxygen atoms. Another possibility is that a fraction of the product bands are cross-linked with each other, but this is unlikely, as such cross-linking would generate additional new bands of high masses in SDS PAGE, which are not observed.

Concentration Dependence, and Excitation at Longer Wavelengths. Photoproduct yields and the selectivity of the photocleavage were monitored as a function of increasing metal complex concentrations (Figure 2). The increase (8–23%, 0.1 – 0.6 mM) is gradual in the case of $[\text{Co}(\text{NH}_3)_5\text{Br}]^{2+}$, and yields increased abruptly with $[\text{Co}(\text{NH}_3)_4\text{CO}_3]^+$, from 12 to 32% (0.5 to 2.5 mM), but no further increases are noted. More importantly, the same two photoproducts are formed at all concentrations, and both indicated no change in reaction selectivity. This latter observation is significant because the addition of excess metal complex increases the concentration of the free metal complex, and if the reaction is due to the free complex, then the selectivity could diminish. On the other hand, if the reaction originates from complexes bound to a particular site on the protein, then the selectivity will not change.

Increased product formation with increases in metal complex concentration deserves some comment. One possibility is that light absorption by the metal complex is the primary photochemical process, and increased product yield is due to increased light absorption. Another possibility is that light absorption by the protein is the primary photochemical process, and quenching of protein-derived

Table 2. A Comparison of Best Yields of Lysozyme Photocleavage by Co(III) Complexes

Co(III) complex	% yield	[Co(III) complex] (mM)	irradiation time (h)	λ_{irr} (nm)	buffer
$[\text{Co}(\text{NH}_3)_5\text{Br}]^{2+}$	43	0.6	0.5	370	TrisHBr
$[\text{Co}(\text{NH}_3)_4\text{CO}_3]^+$	40	5	0.67	370	TrisHCl

excited state(s) by the metal complex initiates product formation. To distinguish between these possibilities, we examined the photo-product yields as a function of irradiation wavelength.¹³

Previous data showed that both $[\text{Co}(\text{NH}_3)_5\text{Br}]^{2+}$ and $[\text{Co}(\text{NH}_3)_4\text{CO}_3]^+$ complexes cleave lysozyme at irradiation wavelengths up to 390 nm. Irradiation of lysozyme at these wavelengths, in the absence of the metal complex, did not give rise to any products (data not shown). Since protein residues have little or no absorption at wavelengths greater than 310 nm, light absorption by the metal complex, but not the protein, is necessary for the product formation.

Our hypothesis is that ligand-derived radicals generated by the photoreduction of the metal complex drive protein cleavage. First, these Co(III) complexes are known to undergo photoreduction (Table 1) with concomitant ligand oxidation.³⁵ Second, the bromo-derivative undergoes photoreduction at wavelengths as long as 550 nm,³⁶ even though the corresponding LMCT band is located at much shorter wavelengths.³⁷ One possibility is that the LMCT bands tail-out into longer wavelengths or that the initially populated LF states sensitize the formation of the triplet LMCT states, and the reaction occurs from these states. Note that, in all cases, at all wavelengths and all metal complex concentrations, the same two product bands were observed. Conditions for the highest photocleavage yields are given in Table 2.

Effect of Oxygen. The role of oxygen in the photocleavage was investigated by purging the reaction mixture with nitrogen gas. The photocleavage was independent of oxygen concentrations, for both the metal complexes. For example, the same yield of product I was noted when the photoreactions were run after saturation with O₂ or when deoxygenated with N₂. Deoxygenation of the sample was tested in a separate experiment, where the fluorescence from a dye added to the sample was monitored as a function of time of degassing and the same conditions applied for degassing the reaction mixtures. Therefore, neither triplet states nor oxygen-sensitive species are involved in the photocleavage, or such species, if present, are very short-lived.

Photocleavage Inhibition by Gd(III). Metal ions such as Ni(II), Zn(II), Ca(II), Cd(II), and Gd(III) bind to the Asp35/Glu52 site at the active site of lysozyme.^{18,20,21} Since we hypothesize that the Co(III) complexes bind at this site and mediate photocleavage, we expected that one or more of these metal ions should inhibit photocleavage.³⁸ Irradiation of a solution of lysozyme (75 μ M), and $[\text{Co}(\text{NH}_3)_4\text{CO}_3]^+$ (2.5 mM, @350 nm, 0.5 h), in the presence of increasing concentrations of Gd(III) and subsequent analysis by SDS PAGE indicated gradual inhibition of the photocleavage. The bands in the gel were quantified, and plots of ϕ_0/ϕ as a function of inhibitor concentration were obtained (Figure 3), where ϕ_0 is the yield of photoproduct I in the absence of quencher, and ϕ is the yield in the presence of quencher.

(35) Pribush, R. A.; Poon, C. K.; Bruce, C. M.; Adamson, A. W. *J. Am. Chem. Soc.* **1974**, *96*, 3027.

(36) Adamson, A. W. *Discuss. Faraday Soc.* **1960**, *29*, 163.

(37) (a) Brasted, R. C.; Hirayama, C. *J. Phys. Chem.* **1959**, *63*, 780. (b) Sastri, V. S. *Inorg. Chim. Acta* **1972**, *6*, 264. (c) Endicott, J. F.; Ferraudi, G. J.; Barber, J. R. *J. Phys. Chem.* **1975**, *79*, 630–. (d) Endicott, J. F.; Hoffman, M. Z. *J. Am. Chem. Soc.* **1965**, *87*, 3348. (e) Sastri, V. S.; Langford, C. H. *Can. J. Chem.* **1969**, *47*, 4237.

(38) Li, S. J. *Biopolymers* **2006**, *81*, 74.

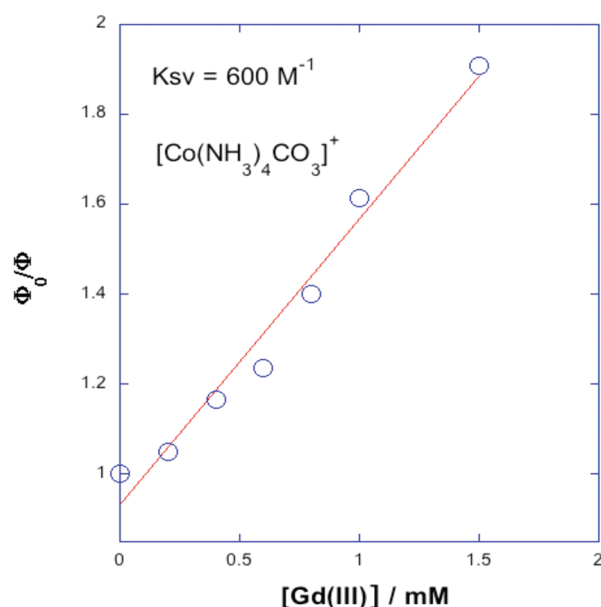


Figure 3. Gd^{3+} quenching of $[\text{Co}(\text{NH}_3)_4\text{CO}_3]^+$ (2.5 mM) induced lysozyme (75 μM) photocleavage (350 nm, 0.5 h). Errors are approximately $\pm 10\%$.

The data were analyzed using the Stern–Volmer equation, $\Phi_0/\Phi = 1 + K_{sv}[Q]$ where K_{sv} is the Stern–Volmer constant ($K_{sv} = k_q\tau$, where τ is the lifetime) and $[Q]$ is the quencher concentration. The best fit to the plot indicated a slope of 600 M^{-1} , and data clearly show that $\text{Gd}(\text{III})$ quenches the photoproduct formation efficiently.

The $\text{Gd}(\text{III})$ quenching of photocleavage is in line with our earlier work where we showed that $\text{Co}(\text{II})$ (10 mM) and $\text{Ni}(\text{II})$ (2 mM) also inhibit the photocleavage of lysozyme and that the reaction is not inhibited by NaCl (up to 300 mM).¹³ Therefore, mere increase in ionic strength is not responsible for the observed inhibition. Molecular modeling studies (Rasmol v. 1.62) confirm that the space around Glu35/Asp52 is adequate to accommodate these small metal complexes on the protein and protein-bound metal complex could be responsible for photocleavage. This hypothesis was further tested in lysozyme activity studies.

Inhibition of Lysozyme Activity. Since Asp52/Glu35 are in the active site of lysozyme and these residues are essential for lysozyme activity, binding of the metal complexes to these residues is expected to inhibit lysozyme activity. Note that $\text{Gd}(\text{III})$ inhibits lysozyme activity by binding to these residues.³⁹ Therefore, we tested the above hypothesis that $\text{Co}(\text{III})$ complexes also bind to this site by testing the activity of lysozyme in the presence of increasing concentrations of $\text{Co}(\text{III})$ complexes.

Activity was followed by a colorimetric method where the hydrolysis product from glycol chitin was used to reduce $\text{K}_3\text{Fe}(\text{CN})_6$ to $\text{K}_4\text{Fe}(\text{CN})_6$, and the extent of metal reduction was quantified by the color change in a colorimetric assay.²⁵ Hydrolysis of chitin was monitored with increasing concentrations (2, 4, and 8 mM) of $[\text{Co}(\text{NH}_3)_4\text{CO}_3]^+$, and activity was inhibited by 27, 45, and 67% at these concentrations, respectively. Therefore, by considering the facts that $\text{Gd}(\text{III})$ inhibits lysozyme photocleavage and that $[\text{Co}(\text{NH}_3)_4\text{CO}_3]^+$ inhibits lysozyme activity, we conclude that the metal complex and $\text{Gd}(\text{III})$ might bind to the protein at the Glu35/Asp52 site. Allosteric interactions, where the metal complex binds elsewhere on the protein and inhibits its

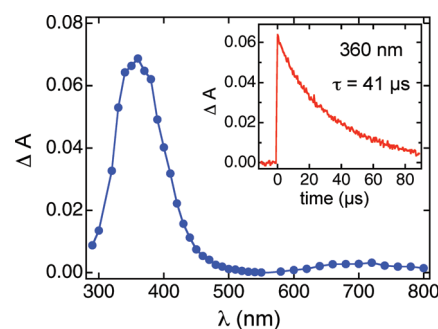


Figure 4. Transient absorption spectrum recorded 0.5–3 μs after laser excitation ($\lambda_{\text{ex}} = 308 \text{ nm}$) of air-saturated aqueous solutions of $[\text{Co}(\text{NH}_3)_5\text{Br}]^{2+}$ (0.4 mM) in Tris HBr (10 mM, pH 7.0). Inset: Decay trace monitored at 360 nm, which followed first-order kinetics with a lifetime of 41 μs .

activity, can not be ruled out. Given this caveat, ligand-derived radicals photogenerated from the protein-bound metal complex are likely responsible for the cleavage reaction. The photogeneration of ligand-derived radicals and their reactivity with lysozyme was examined by laser flash photolysis studies.

Laser Flash Photolysis Studies. Photoexcitation of $[\text{Co}(\text{NH}_3)_6]^{3+}$, $[\text{Co}(\text{NH}_3)_5\text{Cl}]^{2+}$, $[\text{Co}(\text{NH}_3)_5\text{Br}]^{2+}$, and $[\text{Co}(\text{NH}_3)_4\text{CO}_3]^+$ into their respective LMCT bands are known to produce corresponding radical ions, $\text{NH}_3^{\bullet+}$, Cl^\bullet , Br^\bullet , $\text{CO}_3^{\bullet-}$, respectively.⁴⁰ These intermediates have characteristic absorption spectra, lifetimes, and reactivities, which can be monitored in flash photolysis studies. The transients produced in the photocleavage were investigated in time-resolved studies in the presence or absence of lysozyme.

Laser excitation of $[\text{Co}(\text{NH}_3)_5\text{Br}]^{2+}$ (0.4 mM metal complex, 10 mM KBr, 308 nm excitation) resulted in a strong transient absorption spectrum with a peak at 360 nm and a broadband in the region of 700 nm (Figure 4, integrated over a time window of 0.5–3 μs after the laser pulse, air saturated solutions). The decay trace at 360 nm indicated first-order kinetics ($k = 2.4 \times 10^4 \text{ s}^{-1}$), and a lifetime of 41 μs . The decay was independent of the concentration of dissolved oxygen, which indicates that the reactive intermediate is not a triplet state or that the intermediate is unreactive towards oxygen.

Formation of the 360 nm transient is rapid, within the pulse-width of the excitation source (15 ns), and the 700 nm transient also indicated a rapid formation on this time scale, but the intensity of this transient is too weak to obtain a rate constant for its decay. The absorption spectrum shown in Figure 4 (maxima at 360 and 700 nm, in aqueous media) matches well with that reported for $\text{Br}_2^{\bullet-}$ (maxima at 360 and 680 nm, in acetonitrile).⁴¹

Excitation of $[\text{Co}(\text{NH}_3)_5\text{Br}]^{2+}$ at 308 nm is expected to form the singlet LMCT state initially,²⁵ and this may undergo intersystem crossing to $^3\text{LMCT}$. Both these states were proposed to induce homolytic fission of $\text{Co}-\text{Br}$ bond, resulting in the reduction of $\text{Co}(\text{III})$ to $\text{Co}(\text{II})$ and the formation of Br^\bullet .^{9,11} Subsequent reaction of Br^\bullet with Br^- with a rate constant of $9 \times 10^9 \text{ M}^{-1} \text{ s}^{-1}$ gives rise to the rapid formation of $\text{Br}_2^{\bullet-}$.⁴² For example, the reaction of bromine atoms with $\geq 3 \text{ mM}$ Et_4NBr (acetonitrile) resulted in the rapid growth of $\text{Br}_2^{\bullet-}$ which appeared to be within

(39) Secemski, I. I.; Lienhard, G. E. *J. Biol. Chem.* **1974**, *249*, 2932.

(40) (a) Hoffman, M. Z.; Olson, K. R. *J. Phys. Chem.* **1978**, *82*, 2631. (b) Penkett, S. A.; Adamson, A. W. *J. Am. Chem. Soc.* **1965**, *87*, 2514. (c) Chen, S.; Cope, V. W.; Hoffman, M. Z. *J. Phys. Chem.* **1973**, *77*, 1111. (d) Cope, V. W.; Chen, S.-N.; Hoffman, M. Z. *J. Am. Chem. Soc.* **1973**, *95*, 3116.

(41) Scaiano, J. C.; Barra, M.; Krzywinski, M.; Sinta, R.; Calabrese, G. *J. Am. Chem. Soc.* **1993**, *115*, 8340.

(42) Nagarajan, V.; Fessenden, R. W. *J. Phys. Chem.* **1985**, *89*, 2330.

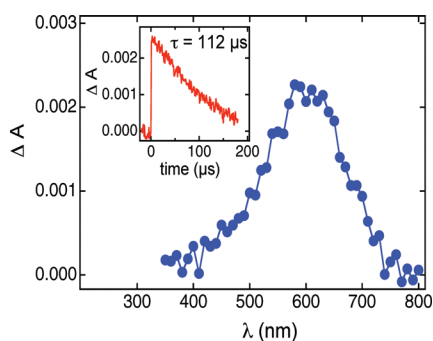


Figure 5. Transient absorbance spectrum of $[\text{Co}(\text{NH}_3)_4\text{CO}_3]^+$ (0.4 mM) in aqueous solutions (Tris HCl 10 mM, pH 7.0), recorded 1–17 μs after laser excitation ($\lambda_{\text{ex}} = 308 \text{ nm}$, air saturated aqueous solutions). Inset: Transient decay trace at 600 nm, which was fitted to a first-order decay with a lifetime of 112 μs .

Table 3. Properties of Transients Observed in the Laser Flash Photolysis (308 nm Excimer Laser) of Co(III) Complexes

complex	λ_{max} of the transient (nm)	k_o (s^{-1})	lifetime (μs)	k_q (lysozyme) ($10^8 \text{ M}^{-1} \text{ s}^{-1}$)
$[\text{Co}(\text{NH}_3)_5\text{Br}]^{2+}$	360, 700	2.4×10^4	41	14
$[\text{Co}(\text{NH}_3)_4\text{CO}_3]^{1+}$	600	8.9×10^3	112	6

the excitation pulse. Therefore, under our experimental conditions, which contained 10 mM bromide, the formation of $\text{Br}_2^{\cdot-}$ is also expected to be complete within the excitation laser pulse, and it is the primary radical intermediate generated in the absence of the protein.

Flash photolysis studies of aqueous solutions of $[\text{Co}(\text{NH}_3)_4\text{CO}_3]^+$ (pH 7.0, 308 nm, air saturated) indicated a weak but longer-lived transient (Figure 5). The absorption spectrum of the transient collected over the time window of 1–17 μs indicated a maximum around 600 nm (Figure 5, Table 3). This transient decayed over a long time with a pseudo-first-order decay of 112 μs , and these features match well with that of carbon trioxide radical ion, which has an absorption maximum at 600 nm (acetonitrile) and a pseudo-second-order decay rate constant of $3.8 \times 10^7 \text{ s}^{-1}$.^{40c,43} Initial photoexcitation was suggested to result in the population of $^1\text{LMCT}$ state, which, after intersystem crossing, undergoes rapid homolytic breaking of the Co–O bond. This results in the opening of the metal chelate ring, followed by the release of $\text{CO}_3^{\cdot-}$. At pH values less than 9, this species was suggested to have been protonated to produce $[\text{CO}_3\text{H}]^{\cdot}$, which can react with a variety of electron-rich substrates to give bicarbonate ion.^{40d}

Photolysis of the metal complexes, under our conditions, generates ligand-derived radicals, and our data are consistent with literature reports. The characteristics of these transients are collected in Table 3. Next we examined the reactivities of these intermediates toward lysozyme, in quenching studies.

Flash photolysis studies of $[\text{Co}(\text{NH}_3)_5\text{Br}]^{2+}$ and $[\text{Co}(\text{NH}_3)_4\text{CO}_3]^+$ in the presence of increasing concentrations of lysozyme caused a decrease in the lifetimes of the respective transients at 360 nm ($\text{Br}_2^{\cdot-}$) and 600 nm ($\text{CO}_3^{\cdot-}$), respectively. Initial absorbance of the transients at the end of the laser pulse did not change with lysozyme concentration (data not shown), but the lifetime of the transients gradually decreased. Decay traces of both the transients at different lysozyme concentrations fit well to a pseudo-first-order decay kinetic model (k_{obs}).

The quenching rate constants (k_q) were determined from the slopes of the plot of the pseudo-first-order rate constants (k_{obs})

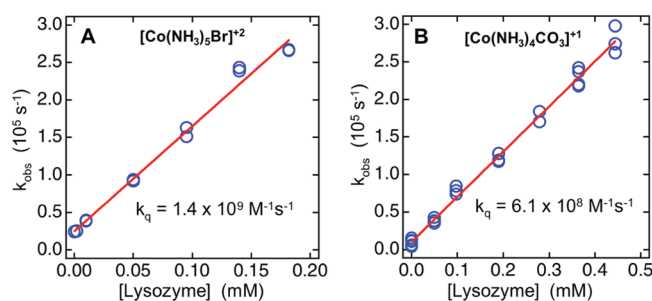


Figure 6. Quenching of transients from $[\text{Co}(\text{NH}_3)_5\text{Br}]^{2+}$ (A) and $[\text{Co}(\text{NH}_3)_4\text{CO}_3]^+$ (B) by lysozyme (10 mM TrisHCl or TrisHBr, pH 7) after laser excitation (308 nm). Dependence of the decay rate constants at 360 nm (A) and 600 nm (B) on lysozyme concentration.

versus the lysozyme concentration (Q) (Figure 6) according to the equation $k_{\text{obs}} = k_o + k_q [Q]$, where k_o is the rate constant in the absence of lysozyme. Quenching rate constants of $1.4 \times 10^9 \text{ M}^{-1} \text{ s}^{-1}$ and $6.1 \times 10^8 \text{ M}^{-1} \text{ s}^{-1}$ were obtained for $\text{Br}_2^{\cdot-}$ and $\text{CO}_3^{\cdot-}$, respectively. The latter value (quenching of $\text{CO}_3^{\cdot-}$ by lysozyme) is in agreement with that reported in the literature ($5.5 \times 10^8 \text{ M}^{-1} \text{ s}^{-1}$).⁴⁴ Note that lysozyme quenches $\text{CO}_3^{\cdot-}$ (600 nm transient) more slowly than $\text{Br}_2^{\cdot-}$ (360 nm transient). Replotting the kinetic data shown in Figure 6, using the Stern–Volmer equation $k_{\text{obs}}/k_o = 1 + K_{\text{sv}} [\text{lysozyme}]$ indicated K_{sv} values of $\sim 7 \times 10^4 \text{ M}^{-1}$ and $6 \times 10^4 \text{ M}^{-1}$ for $\text{Br}_2^{\cdot-}$ and $\text{CO}_3^{\cdot-}$, respectively. These values are nearly consistent with the product of the respective lifetimes and quenching constants.

Quenching of these transients by lysozyme resulted in the formation of protein-derived radical intermediates, and these are probed by recording the time-resolved absorption spectra (Figure 7). Laser excitation of a mixture of $[\text{Co}(\text{NH}_3)_5\text{Br}]^{2+}$ (0.4 mM) and lysozyme (0.12 mM), resulted in the growth of new transients with absorbance maxima at 320 and 510 nm. At the end of the laser pulse, the transient absorption spectrum of $\text{Br}_2^{\cdot-}$ is observed (Figure 7A, blue spectrum, 0.8–1.2 μs after the laser pulse). However, the transient spectrum recorded in a time window of 14–18 μs (Figure 7A, red spectra) showed that the 360 nm transient nearly disappeared, but new peaks at 320 and 510 nm were observable. Consistent with this conclusion, the Trp^{\cdot} spectra formed by pulse radiolysis of tryptophan with $\text{Br}_2^{\cdot-}$ indicated absorption peaks at 320 and 510 nm, and present data are in agreement with literature values.⁴⁵

The 360 nm transient decays simultaneously with the growth of the 510 nm transient (Figures 7B and C). However, there is a significant growth of the 510 nm transient (50%) within the laser pulse-width, indicating that there is a much faster pathway for the production of this transient, or static quenching, which is, in addition to the dynamic quenching mechanism, discussed above. Formation of this portion of the 510 nm intermediate is reproducible, very rapid, and it is distinct from the quenching of $\text{Br}_2^{\cdot-}$ by lysozyme, noted earlier.

The 510 nm transient decays on a very long time scale ($> 500 \mu\text{s}$), and its lifetime could not be determined on our experimental setup. This transient is assigned to radicals generated primarily from Trp, while radicals from other residues such as tyrosine and histidine may also contribute to this transient.⁴⁶ Absorbance of

(44) Chen, S.; Hoffman, M. Z. *Radiat. Res.* **1973**, *56*, 40.

(45) Adams, G. E.; Aldrich, J. E.; Bisby, R. H.; Cundall, R. B.; Redpath, J. L.; Willson, R. L. *Radiat. Res.* **1972**, *49*, 278.

(46) (a) Hsiao, J. S.; Webber, S. E. *J. Phys. Chem.* **1993**, *97*, 8289. (b) Bohne, C.; Abuin, E. B.; Scaiano, J. C. *J. Am. Chem. Soc.* **1990**, *112*, 4226. (c) Hirata, Y.; Mataga, N. *J. Phys. Chem.* **1985**, *89*, 2439. (d) Vala, M.; Szczepanski, J.; Pauzat, F.; Parisel, O.; Talbi, D.; Ellinger, Y. *J. Phys. Chem.* **1985**, *98*, 9187.

(43) Behar, D.; Czapski, G.; Duchovny, I. *J. Phys. Chem.* **1970**, *74*, 2206.

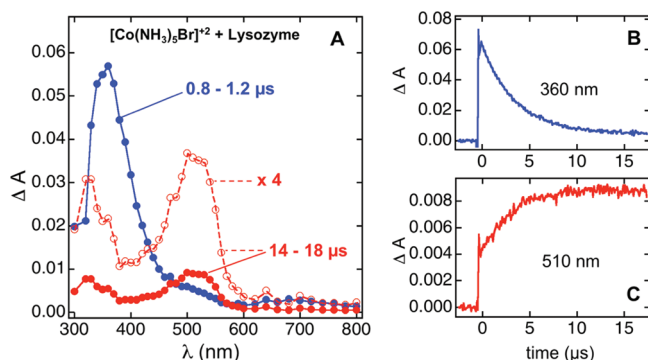


Figure 7. (A) Transient absorption spectra of $[\text{Co}(\text{NH}_3)_5\text{Br}]^{2+}$ (0.4 mM) in the presence of lysozyme (0.12 mM) at 0.8–1.2 μs (blue) and 14–18 μs (red), after the laser pulse ($\lambda_{\text{ex}} = 308$, air saturated Tris buffer pH 7). (B) Decay trace at 360 nm ($\text{Br}_2^{\cdot-}$) and lifetime of 41 μs . (C) Growth of 510 nm transient with a decay time of $>200 \mu\text{s}$.

the 320 nm transient is too weak, and the signal overlaps with ground state absorptions, which makes it difficult to study further. Similar transients (320 and 510 nm) were also noted when $\text{CO}_3^{\cdot-}$ photogenerated from $[\text{Co}(\text{NH}_3)_4\text{CO}_3]^+$ was quenched by lysozyme, but the intensities of these latter transients were much too weak to quantify their properties.

Tryptophan, tyrosine, and histidine residues are known to react with $\text{Br}_2^{\cdot-}$ with rate constants of 7.7×10^8 , 0.2×10^8 , and $0.15 \times 10^8 \text{ M}^{-1} \text{ s}^{-1}$, respectively (22 $^\circ\text{C}$, salt concentration 10^{-1} M , pH ~ 7.5).⁴⁵ These rate constants are slower than that observed for the quenching by lysozyme ($1.4 \times 10^9 \text{ M}^{-1} \text{ s}^{-1}$), and reason for this acceleration with the protein is not clear. One explanation is that, since lysozyme is highly positively charged at neutral pH (pI = 11), the reaction with oppositely charged ion radical would be faster. Note that up to 50% of the 510 nm transient is produced within the laser pulse, and therefore, a considerable amount of Trp radical cation is produced very rapidly (within the excitation pulse). This formation is most likely due to the proximity of the metal complex bound near the Glu35/Asp52 site on the protein, and Trp residues are located near this site. Thus, the steady-state and time-resolved studies strongly suggest that the metal complexes bind to the protein, and the photocleavage reaction arises primarily from the protein-bound metal complex.

Conclusions

The feasibility of protein cleavage by two Co(III) complexes was tested, and they successfully cleave lysozyme at a major site. Photoproduct yield increased with the irradiation time and reached a plateau. This is mainly due to the increased binding of the metal complexes with increased concentration, and the plateau is reached when the binding is saturated. Yields do not

reach 100%; this is often the case with most photoreactions, and rarely are the conversions complete. Addition of fresh metal complex to the partially irradiated reaction mixture did not increase the yield. This clearly shows that the initial photoreaction of the protein branches out to give rise to dead-end products that do not undergo cleavage. Most photoreactions seldom provide 100% conversions to the products because of numerous competing pathways available for the excited states and various intermediates created subsequently. Given these limitations, the yields as high as 43% and high selectivity of just two product bands are remarkable.

Both metal complexes cleaved lysozyme at wavelengths longer than 310 nm, and up to 390 nm. This observation provides strong evidence that light absorption by Trp residues of lysozyme are not responsible for the observed cleavage chemistry. The selectivity of the photoreaction did not change, under a variety of reaction conditions studied here. The Co(III)-induced photocleavage is inhibited by Gd(III), which is known to bind to Glu35/Asp52 at the active site of the enzyme. Binding of the metal complexes to this site is also consistent with inhibition studies, where 8 mM $[\text{Co}(\text{NH}_3)_4\text{CO}_3]^+$ inhibited 70% of the enzyme activity. Taken together, these data strongly suggest that the Co(III) complexes bind to this site on lysozyme and initiate the cleavage reaction. Photocleavage by free metal complexes is unlikely to be responsible for the observed products and is not consistent with the above observations.

The fast growth at 510 nm due to Trp residues, observed in the flash studies, is significant. It implies that the reactive intermediates generated from the metal complexes have a fast access to the Trp residues. Such residues are present within a few angstrom distance from the Gd(III) binding site (Glu35/Asp52), and binding of the metal complexes to this site can result in the observed fast growth of the 510 nm transient. This conclusion is also supported by the steady state data. For example, inhibition of photocleavage by Gd(III) and the inhibition of lysozyme activity by the metal complex support this scenario. All three observations can be explained if the metal complexes bind to the protein, near the active site and initiate protein photocleavage.

Our hypothesis is that the metal complexes bind to Gd(III) binding site in the active site cleft of the enzyme, and protein-bound Co(III) complexes are likely to be responsible for the observed selective photocleavage of lysozyme.

Acknowledgment. We acknowledge the financial support of this work by the National Science Foundation (NSF-DMR-0300631, NSF-DMR-0604815). We thank Mrs. K. Bandara for technical assistance in performing the Gd(III) inhibition and activity studies. The authors at Columbia University thank the National Science Foundation for support through Grants NSF-CHE 04-15516 and NSF-CHE 07-17518.